Analysis of cracks in the welded zone of stainless steel pipe used in high-pressure decomposer equipment

IOP Conf. Series: Materials Science and Engineering **602** (2019) 012063 doi:10.1088/1757-899X/602/1/012063

Analysis of cracks in the welded zone of stainless steel pipe used in high-pressure decomposer equipment

Husaini, M Najib, and I Hasanuddin

Laboratory of Computational Mechanics, Mechanical Engineering Department, Syiah Kuala University, Banda Aceh, Indonesia

E-mail: husainiftm@unsyiah.ac.id

Abstract. ASTM A276 was the material used in a stainless steel pipe inside High-Pressure Decomposer (HPD) equipment that was being used in the fertilizer industry. The pipe had 3 mm of thickness and was operated at a pressure and temperature of approximately 1.7 MPa and 130^0C respectively. Leaking was observed from a crack in a welded area of the Heat Affected Zone (HAZ) and caused the factory to shut down. From the study results, the stress intensity factor (K_I) value at the crack tip was calculated to be approximately 1244 Mpa.m$^{1/2}$, whereas the fracture toughness (K_{IC}) of the pipe material value is 499.9 MPa.m$^{1/2}$. It can be inferred that due to the K_I value being higher than the K_{IC} value, then crack propagation occurred in the welded zone until it penetrated through the pipe wall. The cracking was also influenced by the presence of residual stresses and corrosive fluid flowing in the pipe which produced Stress Corrosion Cracking (SCC). It was further found that the welding process used to join the pipe produced porosity defects, which in turn caused porosity coalescence under the pressure of the pipe in operation, allowing crack propagation to occur and penetration of the pipe wall.

1. Introduction

Welding is a common joining technique used to connect structures. Failure at the join often occurs due to the presence of stress concentrations. The join is also often the weakest point in a structure [1]. With the use of the welding method, the piping system and the joining system are interdependent and cannot be separated from each other. Failures of welded joints in piping systems have been studied [2, 3].

H. M. Shalaby [2] examines a stainless steel pipe that had a crack failure in the weld joint area. The failure happened because the residual stress and the corrosive fluid combined to produce Stress Corrosion Cracking (SCC). Meng-Bi Lin et al. [3], reports that the failures in spiral pipes were caused by residual stresses as a result of the welding and stress concentrations. The result was that cracks easily propagated through the pipe wall. To reduce the problem, proper welding techniques were required to reduce the occurrence of residual stresses. Moreover, a study conducted by Y. Y. Chen et al. [4] indicate that SCC increases with increasing Cl- concentration and causes a decrease in the maximum tensile stress of the material.

Erosion-corrosion was the cause of failure between an elbow and pipe join, as reviewed by Qiao et al. [5]. Erosion-corrosion arises due to fluid flowing in the pipe that is both corrosive and turbulent. The hardness of the surface of the welded area is typically less than the hardness of the pipe base metal surface. The non-uniformity of the mechanical properties of the material in the welded area does not significantly affect the chance of failure of the joint exposed to the erosion-corrosion. However,

the non-uniformity of the geometrical properties in the welded area typically causes failure in the form of erosion-corrosion [6].

The mechanism of crack propagation that occurs in weld metal and welded areas are nearly the same. The welding process does not typically affect crack propagation to failure. The crack propagation properties of the base metal are lower than the welded area [7].

In this study, stainless steel pipes that experienced crack propagation and failure while in operation in High-Pressure Decomposer (HPD) equipment at a fertilizer factory were analyzed. The pipe was operated at a pressure of approximately 1.7 MPa and a temperature of 130^0C. The research aimed to analyse the cause of failure of the pipes that leaked at the weld area. Stress distribution, displacement, and stress intensity factor around the crack tip were analysed by analytical and finite element methods.

2. Method

2.1. Mechanical properties

The pipe material which was used in the HPD equipment is stainless steel, material code ASTM A276. Table 1 shows the mechanical properties of ASTM A276.

Table 1. Mechanical properties of ASTM A276 [8, 9].

No	Description	Value
1	Maximum Tensile Strength, σ_u	655 MPa
2	Yield Strength, σ_y	345 MPa
3	Young's Modulus, E	193 - 200 GPa
4	Hardness, Hv	241 Hv
5	Density, ρ	7740Kg/m^3
6	Poisson Ratio, ν	0.275
7	Fracture Toughness, K_{IC}	499,4 MPa.m$^{1/2}$

2.2. Chemical composition

The chemical composition of ASTM A276 stainless steel pipe is shown in Table 2.

Table 2. Chemical composition of ASTM A276 [8, 9].

Type	Composition (wt %)						
	C	Mn	P	S	Cr	Mo	Si
ASTM A276	0.9	1.0	0.04	0.03	18	0.7	1.0

3. Results and discussions

3.1. Fracture Analysis

Figure 1(a) shows the outside of the stainless steel pipe that was used in the HPD equipment and which experienced a failure due to crack propagation through the pipe wall. This pipe is used for a reboiler piping system the purpose of which is to change *urea slurry* from the liquid phase to gas phase. On the inside, the reboiler pipe had pitting corrosion and erosion-corrosion occurring as shown in Figure 1. Pipes are more susceptible to erosion-corrosion effects in specific areas such as at pipe turns, pipe narrowing areas, and in other areas where the structure changes the velocity and direction of fluid flow [10]. Pitting corrosion is a type of corrosion that often occurs in stainless steel pipes [11, 12]. In addition to the occurrence of pitting and erosion-corrosion, the pipe also experienced Stress Corrosion Cracking (SCC). In general, SCC occurs due to residual stresses, in materials that are susceptible to corrosion, and in corrosive environments [13]. The urea slurry fluid that flows in the stainless steel pipe used in the HPD is corrosive. Also, the welding method used to join the pipe also caused residual stress and increased the occurrence of SCC in this case.

Figure 1. The failure of the stainless steel pipe: (a) The pipe leaked because of crack propagation that penetrated the pipe wall. (b) Porosity observed due to the welding process and pitting corrosion on the inside of the pipe.

A schematic diagram of crack propagation on welded joins is shown in Figure 2. Figure 2(a) is the pipe condition after welding and porosity produced. Figure 2(b) shows crack initiation which is accompanied by coalescence of some porosity due to the increasing stress in the pipe. Crack propagation through the pipe wall occurs with the continued coalescence of porosity as shown in Figure 2(c).

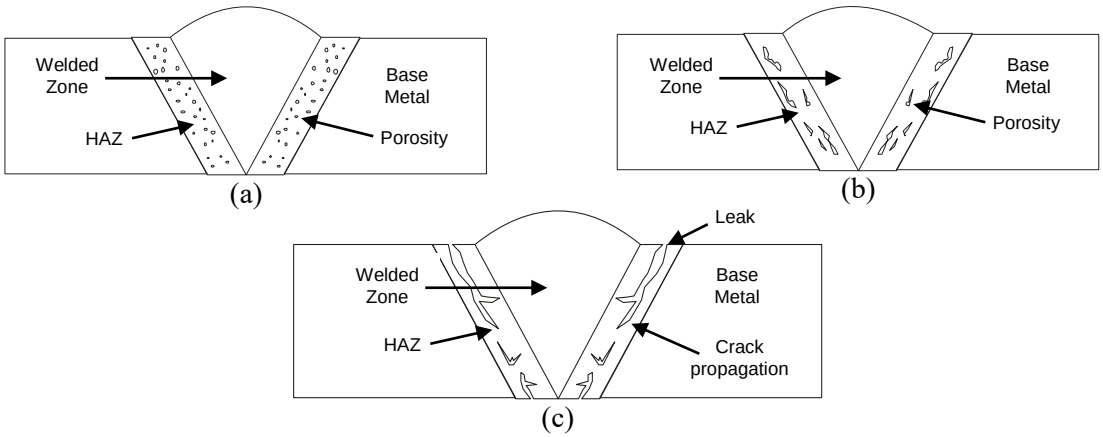

Figure 2. Crack propagation mechanism in the pipe: (a) Welded join that produces porosity. (b) Porosity coalescence and increase in size. (c) Crack propagation through the pipe wall.

3.2. Finite element analysis

Figure 3 shows the modeling of reboiler pipes that were used in the HPD process in 2D and 3D. The pipe model was made using Autodesk Inventor software. The pipe is given a defect with a length of approximately 4 mm and a depth of approximately 2.5 mm. The stress and strain distribution in this pipe was then analyzed by the finite element method.

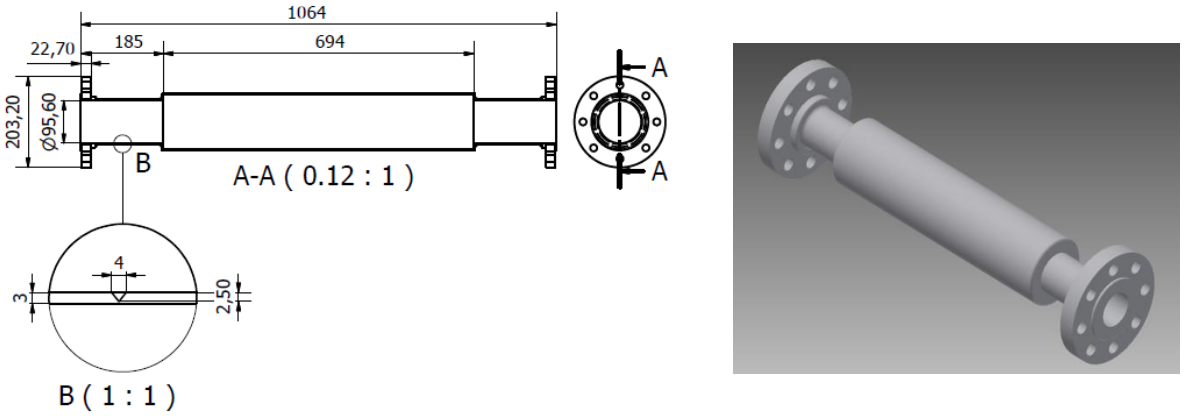

(a) (b)

Figure 3. The modeling of reboiler pipes that used on HPD process in 2D (a) and 3D (b). (unit in mm)

The results of the pipe stress analysis using the finite element method are shown in Figure 4. Figure 4(a) is the stress distribution along the pipe. Figure 4(b) is the inside pipe section where the defect or initial crack occurs. The maximum stress that occurs at the defect is shown in Figure 4(c). It shows that the maximum stress value is approximately 43.29 MPa.

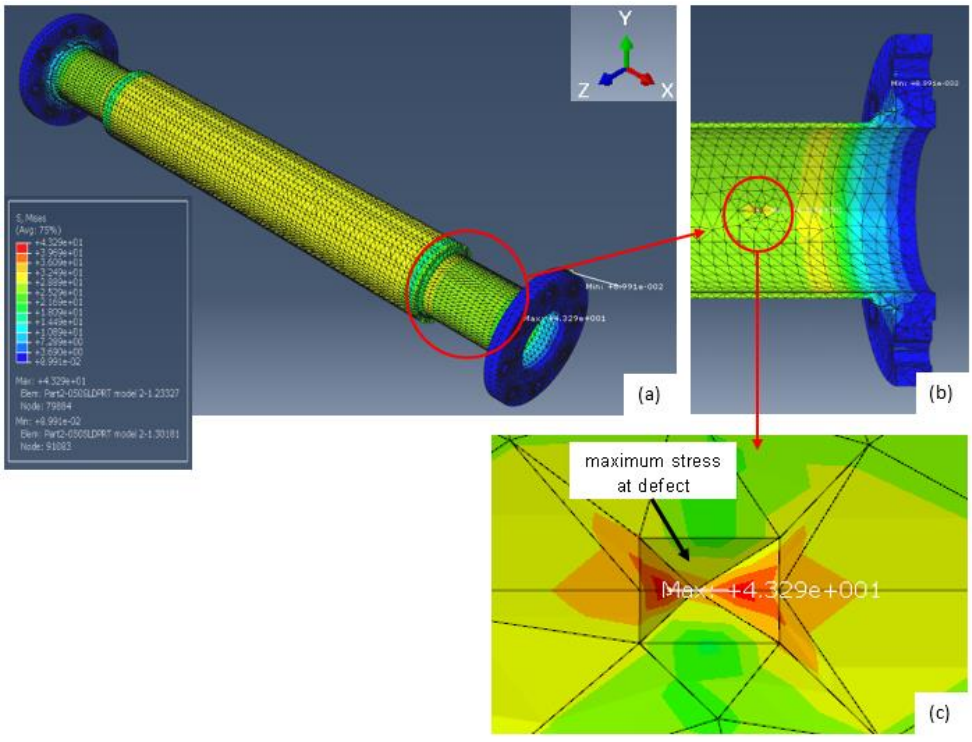

Figure 4. The results of the finite element analysis of the pipe are (a) Stress distribution along the pipe. (b) Finite element mesh modeling with an initial crack at the inside section of the pipe that failed. (c) The maximum stress, occurring at the defect section of the pipe.

The displacement that occurs along the pipe is shown in Figure 5. From the results of the analysis, it can be seen that the maximum displacement occurs at the middle area of the pipe side. The displacement value obtained from the analysis was approximately 1.1 x 10^{-5}m.

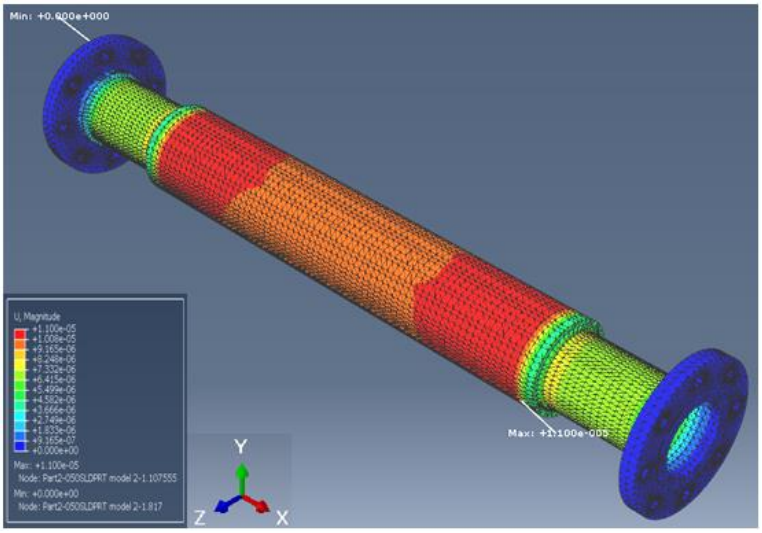

Figure 5. Displacement that occurs along the pipe.

Figure 6(a) it shows the curve of stress and displacement related to the node distance from the crack tip. The node highlighted with a red dot and in a black box (Figure 6 (b)), is the node observed at the crack tip. It can be seen that the stress and displacement value in any region decreases with increasing distance from the crack tip. At the crack tip, the stress value that occurs is approximately 31.2 MPa with a displacement value of approximately 1.5×10^{-5} m.

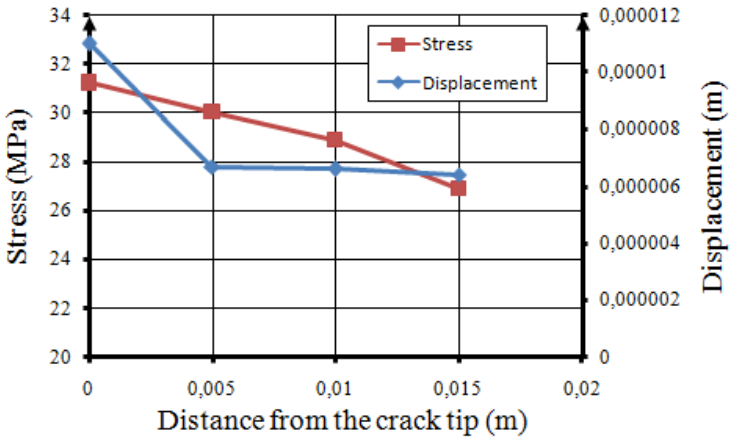

(a)

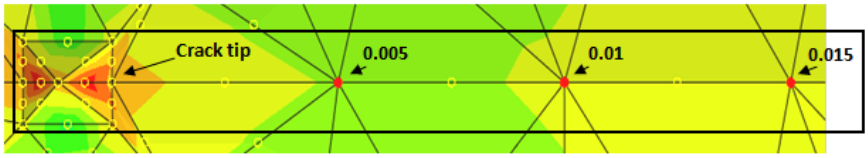

Node distance from the crack tip

(b)

Figure 6. Stress and displacement analysis near the crack tip. (a) Relationship curve between stress and displacement to node distance from the crack tip. (b) The observed node distance from the crack tip.

3.3. Determination of stress intensity factor by analytical analysis

Figure 7 is a C-shaped specimen that is used to determine the value of the stress intensity factor (K_I) by using Equation (1) [14].

$$K_I = \frac{P}{BW^{1/2}}\left[1+1.54\left(\frac{x}{W}\right)+0.5\left(\frac{a}{W}\right)\right]\left[1+0.221\left(1-\left(\frac{a}{W}\right)^{1/2}\right)\left(1-\frac{R_1}{R_2}\right)\right] f\left(\frac{a}{W}\right) \quad (1)$$

$$K_I = 1244 \text{ MPa.m}^{1/2}$$

Where, P is the maximum stress obtained from the finite element analysis (approx. 43.29 MPa), and a is the crack length (approx. 2.5 mm). W is the pipe wall thickness (approx. 3 mm). B is the width of the specimen (approx. 10 mm), and x is the distance from the inside of the pipe to the loading point (approx. 45 mm). R_1 is the inside radius of the pipe (approx. 47.8 mm), and R_2 is the outside radius of the pipe (approx. 50.8 mm). After being calculated using Equation (1), it was found that the KI value is about 1244 MPa.m$^{1/2}$.

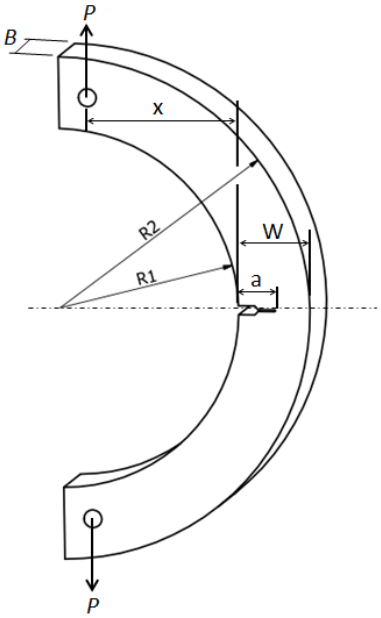

Figure 7. The configuration of the C-shaped specimen.

Based on the analytical result, the value of the stress intensity factor (K_I = 1244 MPa.m$^{1/2}$) obtained is higher than the material fracture toughness (K_{IC} = 499.4 1244 MPa.m$^{1/2}$) of the pipe material, as shown in Table 1. Therefore, this suggests that crack propagation occurring in the welded zone would penetrate the pipe wall. It is known that fracture toughness is affected by the chemical composition of the metal as reported by Akhyar et al. [15]. In non-ferrous metals, studies also show that one of the highly dangerous mechanisms of cracking is when crack propagation occurs in the opening fracture along with fracture in the mixed loading [16-17].

4. Conclusions

The study results about cracking of the stainless steel pipe used in the High-Pressure Decomposer allow the following conclusions to be drawn:

1) Porosity that was produced during the welding process coalesced with crack propagation that occurred due to the increase of stress in the pipe.

2) The stress intensity factor (K_I) value was calculated to be 1244 MPa.m$^{1/2}$, higher than the fracture toughness (K_{IC}) of the pipe material of 499.4 MPa.m$^{1/}$. When $K_I > K_{IC}$, then cracking can easily propagate in the welded zone through the pipe wall.
3) *Stress Corrosion Cracking* (SCC) inside the pipe occurred because urea slurry that flows in the pipe is corrosive and also because of the residual stresses produced by the welding process.

5. Acknowledgment

The authors gratefully acknowledge support from Mr. Muhibbur Rachman who had helped in the data collection of this study. The authors would like to express their gratitude to Syiah Kuala University for financial support for this research through the grant No. 03/UN11.2/PP/PNBP/SP3/2018.

References

[1] ASM International 2002 *ASM Handbook: Welding Brazing and Soldering* (Printed in the United States of America) **6** pp. 15.
[2] Shalaby H M 2017 *Engineering Failure Analysis* **80** pp. 290-298.
[3] Lin M B, Gao K, Wang C J, Volinsky A A 2012 *Engineering Failure Analysis* **25** pp. 160-174.
[4] Chen Y Y, Shih H C, Liou Y M, Wang L H, and Oung J C 2006 *Corrosion* **62** pp. 781-794.
[5] Qiao Q, Cheng G, Li Y, Wu W, Hu H, and Huang H 2017 *Engineering Failure Analysis* **82** pp. 599-616.
[6] Qiao Q, Cheng G, Wu W, Li Y, Huang H, and Wei Z 2016 *Engineering Failure Analysis* **64** pp. 126-143.
[7] Ohta A, Sasaki E, Nihei M, Kosoge M, Kanao M, and Inagaki M 1982 *Int J Fatigue* pp. 223-237.
[8] ASTM International, ASTM A 276–04 2004 *Standard Specification for Stainless Steel Bars and Shapes* (Printed in the United States of America).
[9] Husaini M, Ali M, and Machmud M N 2014 Analisis Kegagalan Daerah Lasan Pipa Stainless Steel Sebagai Media Reboiler Pabrik Pupuk Proceeding Seminar Tahunan Teknik Mesin XIII (SNTTM XIII).
[10] Yang G, Yoon K B, and Moon Y C 2013 *Engineering Failure Analysis* **29** pp. 45-55.
[11] Islam M A and Farhat Z 2017 *Wear* **376-377** pp. 533-541.
[12] Cui Y, Liu S, Smith K, Yu K, Hu H, Jiang W, and Li Y 2016 *Water Research* **88** pp. 816-825.
[13] Martins C M B, Moreira J L, and Martins J I 2014 *Engineering Failure Analysis* **39** pp. 65-71.
[14] Ewalds H L and Wanhill R J H 1986 *International Journal of Metalcasting* **10** pp. 452-456.
[15] Husaini, Kishimoto K, Hanji M, and Notomi M 2016 *ARPN Journal of Engineering and Applied Science* **11** pp. 885-890.
[16] Husaini Z 2016 *International Journal of Technology* **7** pp. 456-462.